LETTER
ATMOSPHERIC PHYSICS

Earth and Planetary Physics
9: 452–459, 2025
doi: 10.26464/epp2025010

Performance of CRA-40 reanalysis in representing the Antarctic winter stratospheric circulation: a comparison with ERA-5 and MERRA-2

ZiXu Wang[1], JingGao Hu[1*], Jing-Jia Luo[1,2], Jian Rao[1], ZongZe Li[1], and LiuChi Yan[3,4]

[1]Key Laboratory of Meteorological Disaster, Ministry of Education (KLME), Joint International Research Laboratory of Climate and Environment Change (ILCEC), Collaborative Innovation Center on Forecast and Evaluation of Meteorological Disasters (CIC-FEMD), Nanjing University of Information Science & Technology, Nanjing 210044, China;

[2]Institute for Climate and Application Research (ICAR), Nanjing University of Information Science and Technology, Nanjing 210044, China;

[3]State Key Laboratory of Numerical Modeling for Atmospheric Sciences and Geophysical Fluid Dynamics (LASG), Institute of Atmospheric Physics, Chinese Academy of Sciences, Beijing 100029, China;

[4]University of Chinese Academy of Sciences, Beijing 100049, China

Key Points:

- The Antarctic winter stratospheric polar vortex appears strongest in MERRA-2, weakest in ERA-5, with CRA-40 in between.
- The discrepancies among the three reanalyses are confined primarily to the period before 1999, and significantly decrease thereafter.
- In characterizing winter circulation in the Antarctic middle and lower stratosphere, CRA-40 performs comparably to ERA-5 and MERRA-2.

Citation: Wang, Z. X., Hu, J. G., Luo, J.-J., Rao, J., Li, Z. Z., and Yan, L. C. (2025). Performance of CRA-40 reanalysis in representing the Antarctic winter stratospheric circulation: a comparison with ERA-5 and MERRA-2. *Earth Planet. Phys.*, *9*(2), 452–459. http://doi.org/10.26464/epp2025010

Abstract: This paper evaluates a representation of winter stratospheric circulation in the Antarctic that is based on CRA-40, a 40-year global reanalysis dataset released by the China Meteorological Administration, and compares it with representations based on two other state-of-the-art reanalysis datasets: the fifth-generation atmospheric reanalysis provided by the European Centre for Medium-Range Weather Forecasts (ERA-5) and the Modern-Era Retrospective analysis for Research and Applications, version 2 (MERRA-2). In terms of climatology, we find that CRA-40 portrays a stronger and colder polar vortex in the middle and lower stratosphere than ERA-5, but a weaker and warmer one than MERRA-2. However, disagreement among the three reanalyses is confined mainly to the period before 1999, and is largely reduced after that time. On the interannual timescale, portrayals of the intensity and area of the 10-hPa polar vortex are quite consistent among the three reanalyses, with correlation coefficients greater than 0.9 between each pair of reanalyses. In addition, the central dates of most sudden stratospheric deceleration (SSD) events at 10 hPa in the three reanalyses differ by less than one day, indicating that CRA-40 is also highly consistent with the other two reanalysis datasets regarding daily evolution. Our analyses suggest that CRA-40 performs comparably to ERA-5 and MERRA-2 in characterizing winter circulation in the Antarctic middle and lower stratosphere.

Keywords: CRA-40; ERA-5; MERRA-2; Antarctic stratosphere; reanalysis intercomparison

1. Introduction

Reanalysis data play a crucial role in atmospheric research, particularly in studies of the stratosphere, for which atmospheric observations are relatively sparse (Parker, 2016). That paucity of relevant data has long been of concern, raising questions about the accuracy of stratospheric circulation derived from reanalysis data. Almost every current atmospheric reanalysis has been assessed to some degree for its ability to represent stratospheric circulation (e.g., Pawson and Fiorino, 1998, 1999; Randel et al., 2004; Manney et al., 2005; Long et al., 2017; Wright and Hindley, 2018; Rao J et al., 2019; Essa et al., 2022). The Stratosphere–troposphere Processes And their Role in Climate (SPARC) even initiated a specialized project known as the SPARC Reanalysis Intercomparison Project for a better understanding of how various reanalyses differ in characterizing the stratospheric circulation (Fujiwara et al., 2017).

CRA-40 is the first Chinese reanalysis dataset, released by the China Meteorological Administration. Since its release, numerous

First author: Z. X. Wang, 202083300591@nuist.edu.cn
Correspondence to: J. G. Hu, jinggaohu@nuist.edu.cn
Received 07 SEP 2024; Accepted 20 NOV 2024.
First Published online 03 JAN 2025.

studies have been conducted to assess its ability to represent atmospheric variables in the troposphere and at the surface (e.g., Zhao B et al., 2019; Liang X et al., 2020; Yang JX et al., 2021; Zhao D et al., 2021; Shen C et al., 2022; Liu ZQ et al., 2023; Shi C and Zhai PM, 2024). However, research evaluating its usefulness in representing the stratosphere has been lacking. Very recently, Wang ZX et al. (2024) found that CRA-40 performs well in characterizing the winter and spring circulation in the middle and lower Arctic stratosphere, but cannot capture the characteristics of the quasi-biennial oscillation in the equatorial stratosphere.

However, previous studies have suggested that there is a higher disagreement among reanalyses in representing the stratospheric circulation in the Antarctic region, compared to the Arctic region, possibly due to the paucity of observation sites on Antarctica and in the surrounding ocean (e.g., Long et al., 2017; Wright and Hindley, 2018; Essa et al., 2022). This motivates us to ponder how well CRA-40 represents the Antarctic stratospheric circulation, which thus is the focus of this study. We find that CRA-40 demonstrates a robust capability to characterize the winter circulation in the middle and lower Antarctic stratosphere.

2. Data and Methods

It has been suggested that recent reanalyses demonstrate superior performance, compared to their earlier versions, across various dimensions (e.g., Long et al., 2017; Essa et al., 2022). In order to evaluate CRA-40, this study compares its use against that of two other state-of-the-art reanalysis datasets: the fifth-generation atmospheric reanalysis provided by the European Centre for Medium-Range Weather Forecasts (ERA-5, Hersbach et al., 2020) and the Modern-Era Retrospective analysis for Research and Applications, version 2 (MERRA-2, Gelaro et al., 2017). The data compared cover the period from 1 December 1980 to 30 November 2019, with a 1° × 1° horizontal resolution and eight pressure levels (200, 100, 70, 50, 30, 20, 10, and 5 hPa). Table S1 shows a brief summary of the main characteristics of the selected reanalyses. We focus on evaluating CRA-40's performance in the lower (100, 70, and 50 hPa) and middle (30, 20, and 10 hPa) stratosphere due to significant discrepancies among current reanalyses in their upper stratosphere data. However, for comparison purposes we do include one specific pressure level (5 hPa) in the upper stratosphere.

We examine two indicators, the intensity and area, of the stratospheric polar vortex in the Southern Hemisphere. We first identify the edge of the polar vortex in each winter, based on the climatological winter-mean geopotential height at 10 hPa and 60°S. The vortex intensity is defined as the averaged zonal wind along the vortex edge; the vortex area is calculated using the following formula:

$$S = \frac{\pi R^2}{180} \sum_{i=1}^{360} \left(1 - \sin|\varphi_i|\right), \tag{1}$$

where φ is the latitude of the northern edge of the Antarctic polar vortex, R is the radius of the Earth, and S represents the vortex area. In this study, winter in the Southern Hemisphere is defined as June through August, and in the Northern Hemisphere as December through February.

We also examine how well sudden stratospheric warming (SSW) events are captured in CRA-40. Due to the relatively infrequent appearance of major SSW events in the Southern Hemisphere, however, we use sudden stratospheric deceleration (SSD) events to identify Antarctic SSWs. We first compute the anomaly of zonal-mean zonal wind (hereinafter referred to as Ua) by removing the zonal wind's seasonal cycle from the original data. For each day, we then calculate the difference of Ua at 10 hPa and 60°S between five days prior to that day and five days following it; this is termed the "10-day deceleration" for that particular day. Following Birner and Albers (2017) and Yang PK et al. (2023), the "onset" of a possible SSD event is identified when a 10-day deceleration exceeds 27 m·s^{-1}. This threshold is approximately twice the standard deviation of the zonal wind in the daily May–September data record from 1981 to 2019. The "central date" of a qualifying SSD event is defined as the day on which the *maximum* value of deceleration occurs *within a 20-day window that commences on the day of onset*; the "intensity" of the SSD event is taken to be equal to that maximum deceleration value, reached on the event' s central date. It is also stipulated that there must be a minimum interval of 20 days between the central dates of two consecutive SSDs; if this criterion is not met, the candidate SSD with the lower intensity is not counted.

3. Results

3.1 Climatology

We first evaluate the climatology of the austral winter stratospheric polar vortex among the three reanalyses. Figure 1 shows the height–latitude cross sections of the climatological zonal-mean zonal wind in winter in the Southern Hemisphere in the three reanalyses, as well as the differences between each pair of reanalyses. For ease of comparison, we also show the stratospheric circulation in the Northern Hemisphere.

The three reanalysis datasets have a high degree of consistency in characterizing the climatological-mean stratospheric polar night jet in the Northern Hemisphere; biases below 10 hPa between each pair of reanalyses are within ±0.5 m·s^{-1} (Figures 1j–l). This is consistent with findings in Wang ZX et al. (2024). In contrast, the biases increase noticeably in the Southern Hemisphere (Figures 1g–i), which are also consistent with previous studies (e.g., Long et al., 2017; Wright and Hindley, 2018; Essa et al., 2022). We note that the climatological stratospheric polar night jet in the Southern Hemisphere based on MERRA-2 data is strongest; the night jet based on ERA-5 data is weakest. The differences between these two reanalyses at the stratospheric levels above 20 hPa are significant at the 95% confidence level (Figure 1i). Though the main differences between CRA-40 and the other two reanalyses are also concentrated above 20 hPa, they are statistically insignificant (Figures 1g–h). There is a westerly bias of 0.47 m·s^{-1} in the polar night jet's strength over 10–30 hPa and 50°–70°S in CRA-40 when compared to ERA-5, and an easterly bias of −0.57 m·s^{-1} when compared to MERRA-2.

The differences of climatological-mean polar temperature in the Southern Hemisphere among the three reanalyses agree with those of the zonal wind, but they are more significant (Figures 2g–i). Correspondingly, MERRA-2 data deliver the coldest Antarctic

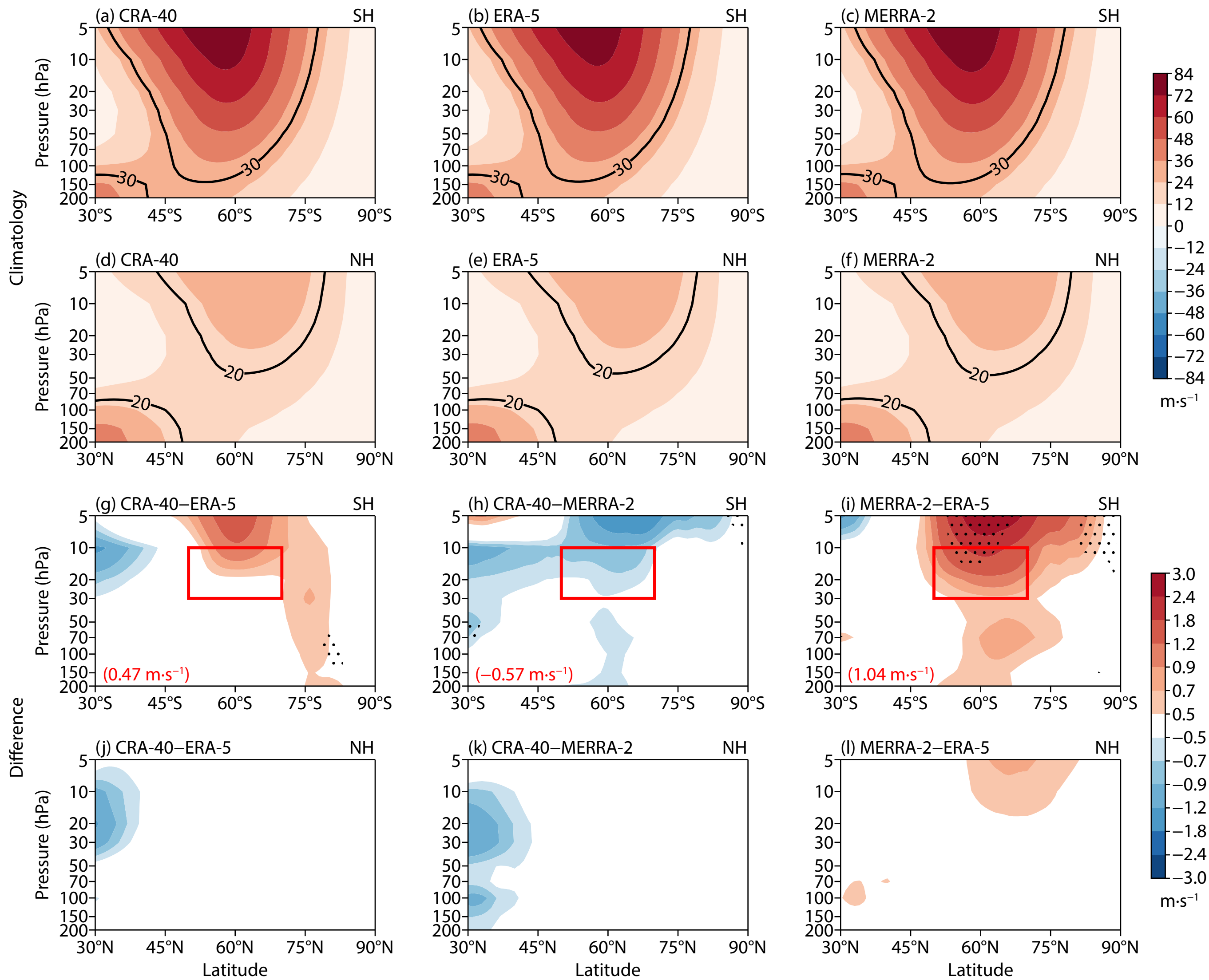

Figure 1. (a–f) Height-latitude cross sections of the climatological zonal-mean zonal wind in winter during 1981–2019 in (a–c) the Southern Hemisphere and (d–f) Northern Hemisphere; (a) and (d) display CRA-40 reanalysis; (b) and (e) display ERA-5; (c) and (f) display MERRA-2. (g–l) As in (a–f), but for the differences (g) and (j) between CRA-40 and ERA-5; (h) and (k) between CRA-40 and MERRA-2; (i) and (l) between MERRA-2 and ERA-5. The dotted areas indicate differences that are significant at the 95% confidence level (based on a two-tailed Student's t-test, and the same below). Values in parentheses in (g–i) represent the differences observed between 50°–70°S (outlined by the red boxes), averaged over 10–30 hPa.

stratospheric polar vortex; ERA-5 data portray the warmest. The bias averaged over 10–30 hPa and 60°–90°S between them reaches −1.32 K (Figure 2i). The strength of the climatological polar temperature in CRA-40 falls between those of MERRA-2 and ERA-5. In the Northern Hemisphere, the biases among the three reanalyses are relatively small and within ±0.5 K in the stratosphere below 10 hPa (Figures 2j–l).

We also investigate the ratio of differences between pairs of reanalysis datasets relative to polar vortex strength. With regard to climatological temperature in the region 10–30 hPa over the polar regions (defined as 60°–90°S and 0–360° in the Southern Hemisphere; 60°–90°N and 0–360° in the Northern Hemisphere), the difference ratios between datasets in the Southern Hemisphere exceed those in Northern Hemisphere datasets (figures not shown).

3.2 Interannual Variations

Next, we compare the interannual variations of the stratospheric polar vortex among the three reanalyses. Figure 3 shows the height–temporal evolution of temperature difference over the polar cap (60°–90°S, 0–360°) in each month from June to August for 1981–2019 between each pair of reanalyses. Over the entire 39-year period, MERRA-2 exhibits a colder polar vortex in the middle and lower stratosphere, except near 50 hPa, compared to ERA-5 and CRA-40, with larger biases in the middle stratosphere than in the lower stratosphere (middle and right panels in Figure 3). However, there is an obvious interdecadal change in the biases between each pair of reanalyses since 1999. During 1999–2019, the biases of winter polar temperature in the middle stratosphere between CRA-40 and ERA-5, between CRA-40 and MERRA-2, and between MERRA-2 and ERA-5 are largely reduced to 18%, 26%, and 24%, respectively, of those observed during 1981–1998. This

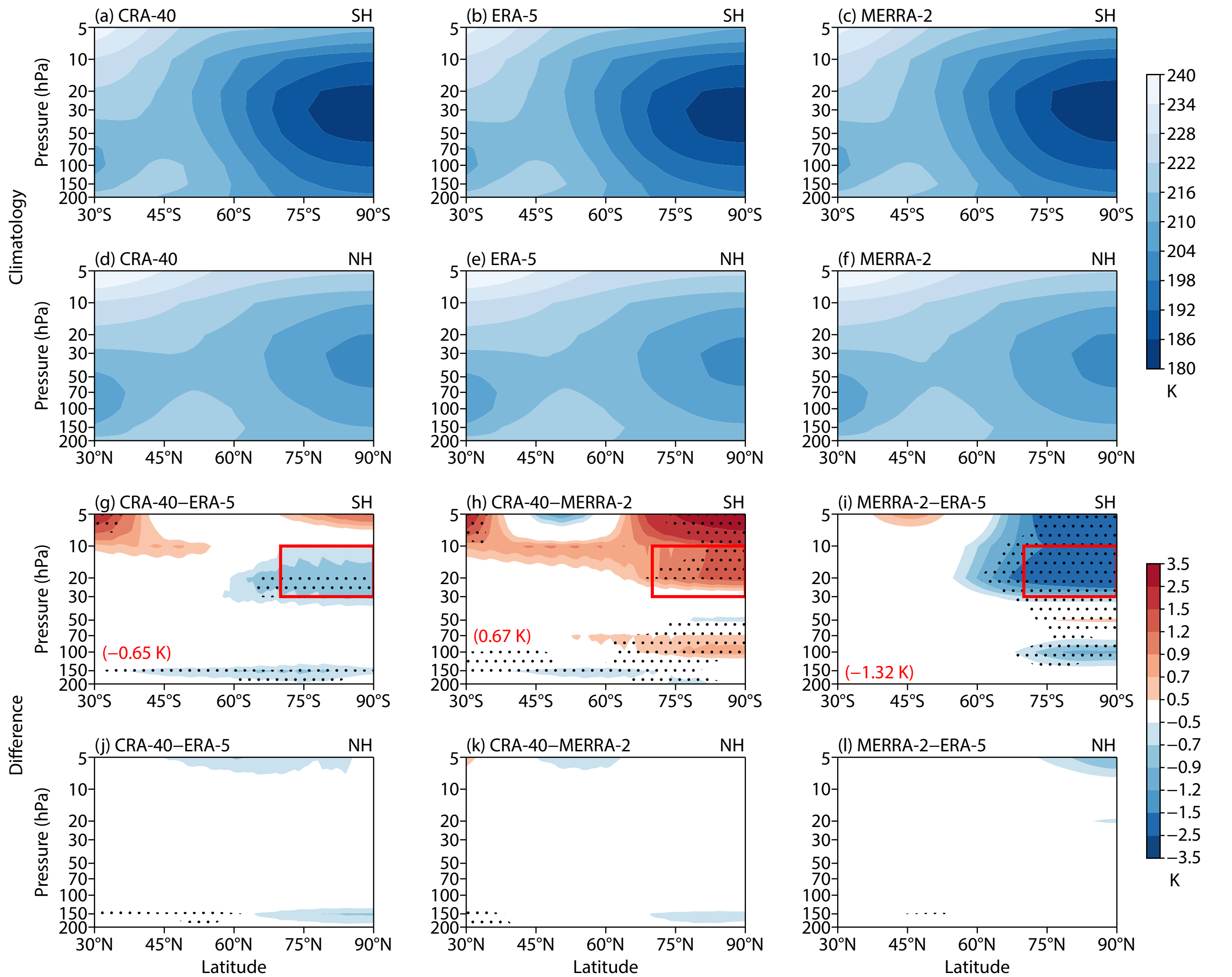

Figure 2. As in Figure 1, but for the climatological zonal-mean temperature. Red boxes indicate the area over 10–30 hPa and 60°–90°S.

significant interdecadal change also exists in the Northern Hemisphere. It has been attributed mainly to the transition of observations from the Stratospheric Sounding Unit (SSU) in the TOVS [Television Infrared Observation Satellite (TIROS) Operational Vertical Sounder] suite of instruments to observations from the Advanced Microwave Sounding Unit-A (AMSU-A) in the ATOVS (Advanced TIROS Operational Vertical Sounder) suite of sounding instruments (Long et al., 2017; Wang ZX et al., 2024).

Additionally, it is worthy of note that during the period 1989–1995, peculiar warm biases (up to ~14 K) occur in the upper stratosphere as derived from CRA-40 data (left and middle panels in Figure 3). We suspect that the lack of assimilation of SSU data may be a reason for this phenomenon. The radiance channels on SSU served as a major source of stratospheric information during the 1980s and 1990s. Both ERA-5 and MERRA-2 assimilate the SSU observations, but CRA-40 does not include the radiance data from SSU (Liu ZQ et al., 2023). This could lead to large biases in the upper stratosphere when CRA-40 is used, compared to ERA-5 and MERRA-2, before the late 1990s. Additionally, the atmospheric forecast model used by CRA-40 is a global spectral model (GSM version 14) from the National Centers for Environmental Prediction (NCEP, Table S1). It has been documented that an earlier version of the NCEP global forecast system model, utilized in the Climate Forecast System Reanalysis, exhibits a notable warm bias in the upper stratosphere prior to 1998 (Long et al., 2017). Therefore, it is plausible that the atmospheric forecast model used in CRA-40 also contributes to this issue. We note that the exact cause of these warm biases remains uncertain and warrants further investigation in future studies.

Figures 4a and 4c further show the annual intensity and area of the 10-hPa stratospheric polar vortex in austral winter for 1981–2019. The interannual variation of both the polar vortex intensity and area exhibit a high agreement among the reanalyses; correlation coefficients between each pair of reanalyses are greater than 0.9. However, a temporal discontinuity is evident in 1999, especially in the differences between CRA-40 and ERA-5 and between MERRA-2 and ERA-5 (Figures 4b, d). The difference of the average intensity of polar vortex between ERA-5 and MERRA-2 is significant at the 95% confidence level (Figure 4b). In CRA-40, both the polar vortex intensity and area are closer to those in MERRA-2

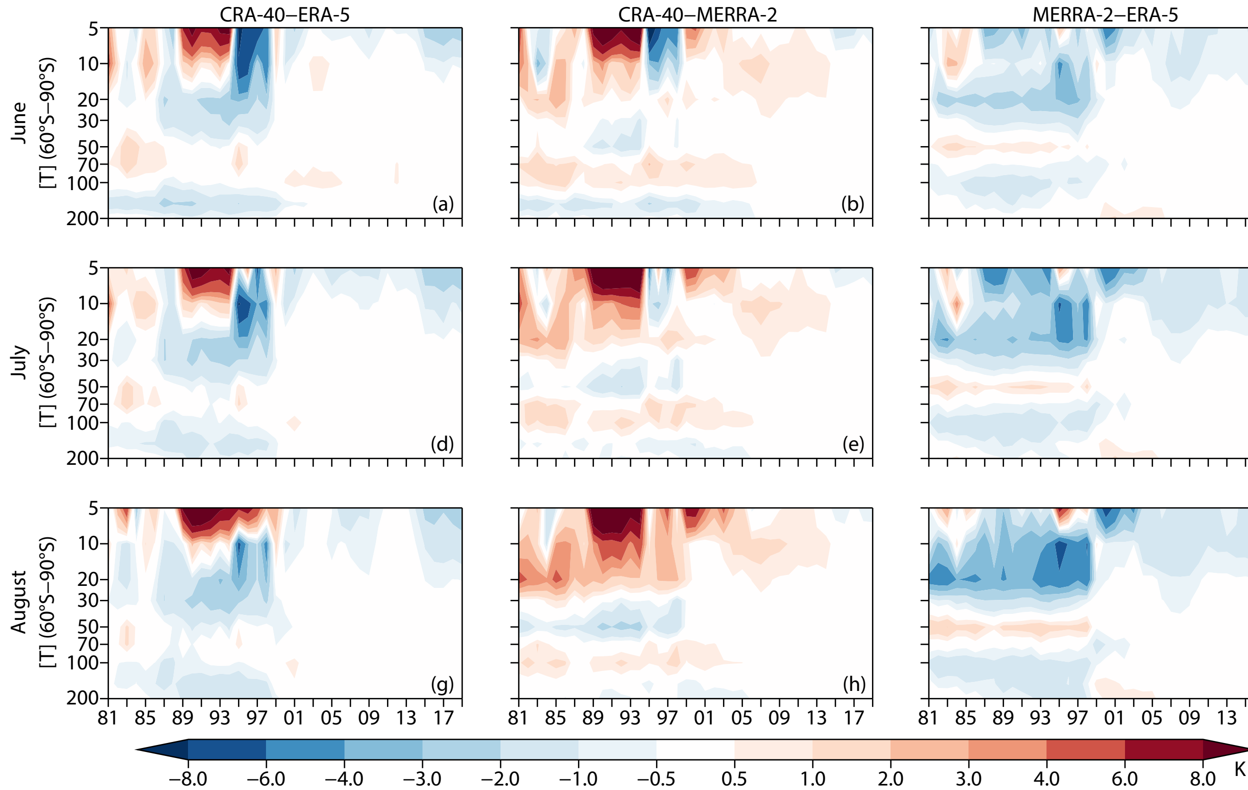

Figure 3. The height–temporal evolution of difference of temperature over the polar cap (60°–90°S, 0–360°) in (a–c) June, (d–f) July, and (g–i) August of 1981–2019: left panels compare CRA-40 to ERA-5; middle panels compare CRA-40 to MERRA-2; right panels compared MERRA-2 to ERA-5.

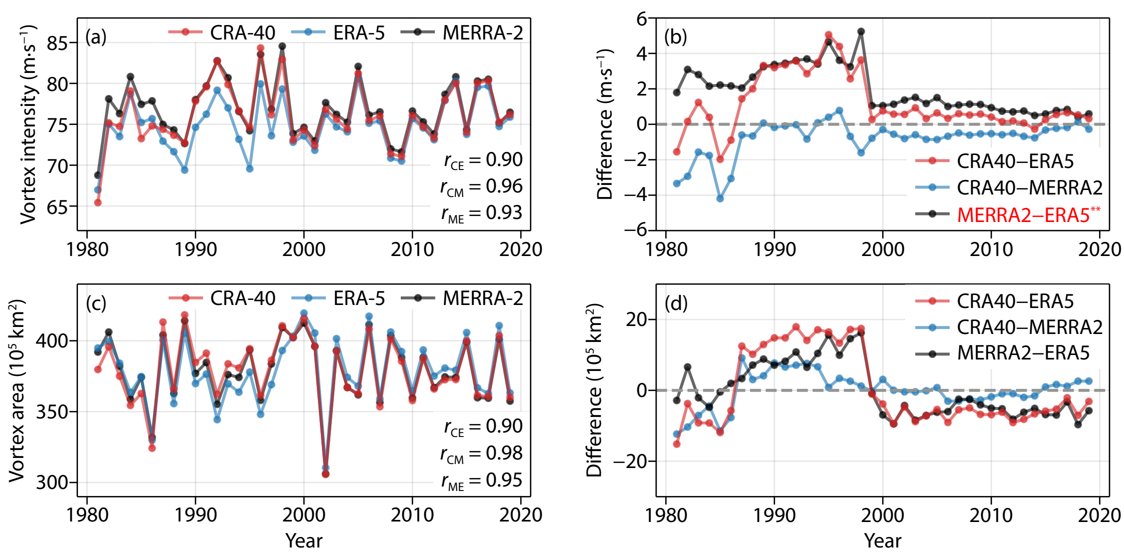

Figure 4. The annual (a) vortex intensity and (c) vortex area in the three reanalyses in austral winter for 1981–2019. The correlation coefficients between CRA-40 and ERA-5 (r_{CE}), between CRA-40 and MERRA-2 (r_{CM}), and between MERRA-2 and ERA-5 (r_{ME}) are given at the lower right corner of each panel. (b, d) as in (a, c), but for the differences between CRA-40 and ERA-5 (red line), between CRA-40 and MERRA-2 (blue line), and between MERRA-2 and ERA-5 (black line). The double asterisks in (b) indicate that the difference of climatological mean is significant at the 95% confidence level.

compared to ERA-5.

3.3 SSD Events

Significant differences among different reanalyses are often found during the onset of major SSWs (Wright and Hindley, 2018). We now turn our attention to SSD events in the Southern Hemisphere. Figure 5a shows the central dates of all SSDs during 1981–2019. Of the total of 34 SSDs, 31 are identified in all three reanalyses; the exceptions are events in 1985, 1987, and 1995. The discrepancies between reanalyses in identifying SSDs amount are due to slight variations in the peak magnitude of deceleration recorded near the threshold. For example, the SSD event in October 1987 is identified only by MERRA-2, which delivers a 10-day maximum deceleration of 27.6 m·s^{-1}; CRA-40 reports the maximum zonal wind deceleration for this event as 26.5 m·s^{-1}, close to the ERA-5 value of 26.1 m·s^{-1}, both of which are less than 1 m·s^{-1} below the threshold that defines an SSD event. We also note that 24 of the 31 SSDs that are identified by all three reanalyses have the same central dates, and the bias of the remaining seven events is only one day. These findings indicate a high agreement of the three reanalyses in identifying the SSDs.

Figures 5b–d present scatter plots of SSD intensity differences against the difference ratios between each pair of reanalyses, which are defined as the difference of SSD intensity divided by the mean intensity over the three reanalyses. Similar to the polar vortex intensity in Figure 4, MERRA-2 reports the strongest SSDs, followed by CRA-40; ERA-5 reports the weakest. An interdecadal change is also observed. During 1981–1998, the averaged SSD intensity biases of MERRA-2 relative to CRA-40 and to ERA-5 reach 1.21 m·s^{-1} and 1.59 m·s^{-1}, respectively, whereas they reduce to 0.18 m·s^{-1} and 0.53 m·s^{-1} during 1999–2019 (Figures 5c–d). However, the bias of SSD intensity between CRA-40 and ERA-5 is relatively small (<0.4 m·s^{-1}) and is steady in both of the two subperiods (Figure 5b). There is also an evident improvement in the difference ratio of the SSD intensity among the reanalyses after the interdecadal change. The maximum difference ratio drops from over 9% in the former subperiod to ~4% in the latter subperiod. Nonetheless, we note that these differences and difference ratios in the SSD intensity among the three reanalyses are insignificant even at the 90% confidence level. The warming events also occur when the stratospheric polar vortex breaks down during austral spring, a phenomenon referred to as *stratospheric final warming* (SFW, Black and McDaniel, 2007). We find that CRA-40 can well characterize the onset process of austral spring SFWs, especially at and below 20 hPa (figures not shown).

4. Summary and Discussion

This study evaluates the applicability of CRA-40 in characterizing the Antarctic winter stratospheric circulation, by comparing it with ERA-5 and MERRA-2 reanalyses. The main conclusions are as follows.

(1) There is a higher disagreement in describing the winter stratospheric polar vortex in the Southern Hemisphere among the three reanalyses compared with that in the Northern Hemisphere. The climatological mean polar westerly jet in the middle and lower stratosphere in CRA-40 is stronger (weaker) than that in ERA-5 (MERRA-2) with a bias of approximately 0.5 m·s^{-1} (−0.6 m·s^{-1}) over 10–30 hPa and 50°–70°S. Meanwhile, the climatological mean temperature in the polar stratosphere is colder (warmer) than that in ERA-5 (MERRA-2) with a bias of approximately −0.7 K (0.7 K) over 10–30 hPa and 60°–90°S.

(2) On the interannual time scale, CRA-40 exhibits a high agreement with the other two reanalyses regarding the temporal evolution of winter vortex intensity and vortex area at 10 hPa. The correlation coefficients between each pair of reanalyses can reach 0.9. However, compared with ERA-5, the vortex intensity and vortex area in CRA-40 are closer to those in MERRA-2.

(3) During 1981–2019, only three winters show discrepancies

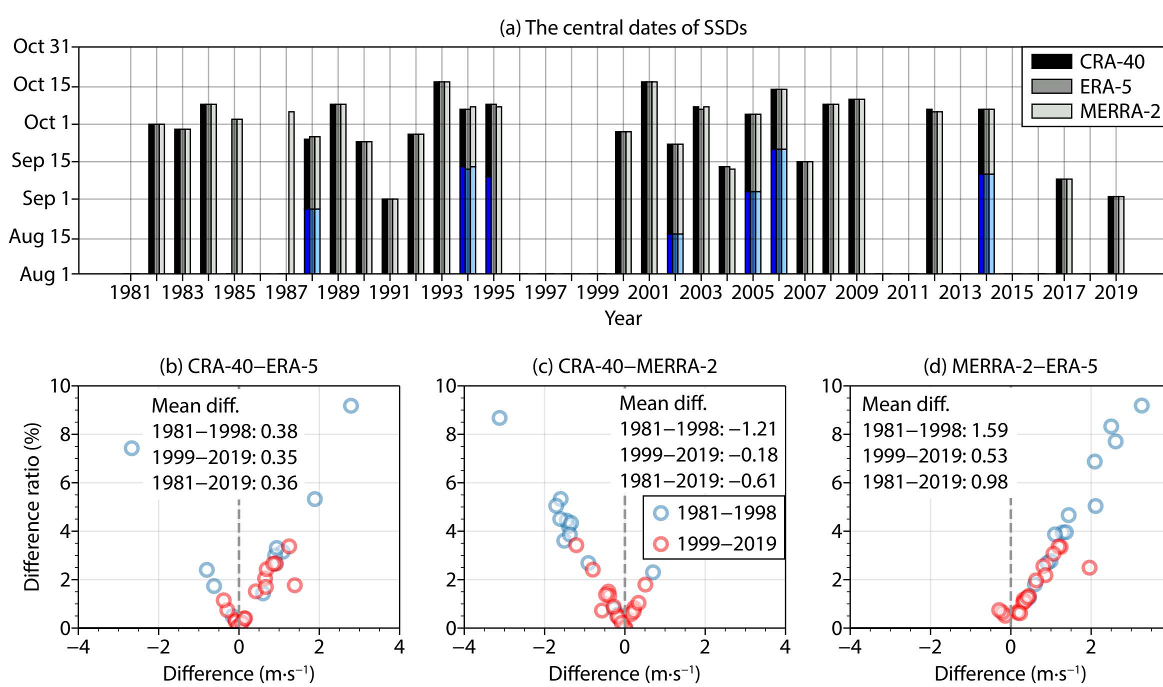

Figure 5. (a) The annual central dates of SSD events during 1981–2019 in the three reanalysis datasets. The dark and light blue bars mark the first SSD event in each year with more than one SSD event. (b–d) The scatter plot of the difference of SSD intensity against the difference ratio (b) between CRA-40 and ERA-5, (c) between CRA-40 and MERRA-2, and (d) between MERRA-2 and ERA-5. The blue circles represent the SSDs during 1981–1998; the red, the SSDs during 1999–2019.

among the three reanalyses in identifying whether an SSD event occurred, which is due to minor biases of wind speed near the threshold. Furthermore, out of 31 SSDs that can be identified by all the three reanalyses, 24 events have consistent central dates, while the remaining seven events differ by no more than one day.

(4) The differences of almost all the selected indicators of the polar stratospheric circulation between each pair of reanalyses show a temporal discontinuity since 1999, which may be due to the transition from the TOVS to ATOVS observations. Compared to that during the subperiod 1981–1998, the disagreement among the three reanalyses largely reduces during the subperiod 1999–2019.

This study does not attempt to determine which reanalysis is more accurate, as we did not compare reanalysis results to observations. In fact, there has always been a debate about which reanalysis is more reliable. For example, Friedrich et al. (2017) concluded that the stratospheric wind in the Southern Hemisphere in MERRA-2 is more accurate because of MERRA-2's enhanced representation of gravity wave drag intensity, while Long et al. (2017) argued that the gravity wave parameterization in MERRA-2 is overly aggressive. Nevertheless, our findings indicate that, overall, CRA-40's ability to represent the Antarctic winter circulation in the middle and lower stratosphere falls between that of ERA-5 and MERRA-2. Considering that the latter two reanalyses represent the latest generation of atmospheric reanalysis data and are widely used in studies of the stratosphere in the Southern Hemisphere, we suggest that CRA-40 demonstrates an excellent performance in characterizing the winter circulation in the middle and lower Antarctic stratosphere.

In addition, all three reanalyses show a greater disagreement in the upper stratosphere than in the middle and lower stratosphere. Particularly, during 1989–1995, there are peculiar warm biases in the upper stratosphere in CRA-40 (up to 14 K) compared to the other two reanalyses. The detailed reason for this warrants our attention in future work.

Acknowledgments

This work is jointly supported by the NSFC project (42088101, 41975048, 42361144843, 42175069). CRA-40 data were downloaded from the web site http://data.cma.cn/data/cdcdetail/dataCode/NAFP_CRA40_FTM_DAY.html. ERA-5 data were downloaded from the web site https://cds.climate.copernicus.eu/cdsapp#!/dataset/reanalysis-era5-pressure-levels?tab=form. MERRA-2 data were downloaded from https://disc.gsfc.nasa.gov/datasets?project=MERRA-2. The authors have no relevant financial interests to disclose.

Supplementary Materials

Table S1. Summary of the main characteristics of the selected reanalyses.[a]

Reanalysis dataset	Model name	Main satellite instruments used in the stratosphere	Data assimilation algorithm	Main reference
CRA-40	NCEP GSM version 14	MSU, AMSU-A, AIRS, IASI, GPSRO	3DVar-FGAT	Liu et al. (2023)
ERA-5	IFS version Cy41r2 (2016)	SSU, MSU, AMSU-A, AIRS, IASI, GPSRO, MLS	4DVar	Hersbach et al. (2020)
MERRA-2	GEOS-5.12.4 (2015)	SSU, MSU, AMSU-A, AIRS, IASI, GPSRO, MLS	3DVar with incremental updating	Gelaro et al. (2017)

[a] Major abbreviation in Table S1:
3DVar, three-dimensional variational (4DVar for four-dimensional variational);
AIRS, Advanced Infrared Sounder;
FGAT, First guess at appropriate time;
GEOS, Goddard Earth Observing System;
GPSRO, Global positioning system radio occultation;
IASI, Infrared Atmospheric Sounding Interferometer;
IFS, Integrated Forecasting System;
MLS, Microwave Limb Sounder.

References

Birner, T., and Albers, J. R. (2017). Sudden stratospheric warmings and anomalous upward wave activity flux. *SOLA*, *13A*, 8–12. https://doi.org/10.2151/sola.13A-002

Black, R. X., and McDaniel, B. A. (2007). Interannual variability in the Southern Hemisphere circulation organized by stratospheric final warming events. *J. Atmos. Sci.*, *64*(8), 2968–2974. https://doi.org/10.1175/JAS3979.1

Essa, Y. H., Cagnazzo, C., Madonna, F., Cristofanelli, P., Yang, C. X., Serva, F., Caporaso, L., and Santoleri, R. (2022). Intercomparison of atmospheric upper-air temperature from recent global reanalysis datasets. *Front. Earth Sci.*, *10*, 935139. https://doi.org/10.3389/feart.2022.935139

Friedrich, L. S., McDonald, A. J., Bodeker, G. E., Cooper, K. E., Lewis, J., and Paterson, A. J. (2017). A comparison of Loon balloon observations and stratospheric reanalysis products. *Atmos. Chem. Phys.*, *17*(2), 855–866. https://doi.org/10.5194/acp-17-855-2017

Fujiwara, M., Wright, J. S., Manney, G. L., Gray, L. J., Anstey, J., Birner, T., Davis, S., Gerber, E. P., Harvey, V. L., … Zou, C. Z. (2017). Introduction to the SPARC Reanalysis Intercomparison Project (S-RIP) and overview of the reanalysis systems. *Atmos. Chem. Phys.*, *17*(2), 1417–1452. https://doi.org/10.5194/acp-17-1417-2017

Gelaro, R., McCarty, W., Suárez, M. J., Todling, R., Molod, A., Takacs, L., Randles, C. A., Darmenov, A., Bosilovich, M. G., … Zhao, B. (2017). The modern-era retrospective analysis for research and applications, version 2 (MERRA-2). *J. Climate*, *30*(14), 5419–5454. https://doi.org/10.1175/jcli-d-16-0758.1

Hersbach, H., Bell, B., Berrisford, P., Hirahara, S., Horányi, A., Muñoz-Sabater, J., Nicolas, J., Peubey, C., Radu, R., … Thépaut, J. N. (2020). The ERA5 global reanalysis. *Quart. J. Roy. Meteor. Soc.*, *146*(730), 1999–2049, https://doi.org/10.1002/qj.3803

Liang, X., Jiang, L. P., Pan, Y., Shi, C. X., Liu, Z. Q., and Zhou, Z. J. (2020). A 10-Yr global land surface reanalysis interim dataset (CRA-Interim/Land):

Implementation and preliminary evaluation. *J. Meteor. Res.*, *34*(1), 101–116, https://doi.org/10.1007/s13351-020-9083-0

Liu, Z. Q., Jiang, L. P., Shi, C. X., Zhang, T., Zhou, Z. J., Liao, J., Yao, S., Liu, J. W., Wang, M. Y., … Hu, K. X. (2023). CRA-40/Atmosphere—The first-generation Chinese atmospheric reanalysis (1979–2018): System description and performance evaluation. *J. Meteor. Res.*, *37*(1), 1–19. https://doi.org/10.1007/s13351-023-2086-x

Long, C. S., Fujiwara, M., Davis, S., Mitchell, D. M., and Wright, C. J. (2017). Climatology and interannual variability of dynamic variables in multiple reanalyses evaluated by the SPARC Reanalysis Intercomparison Project (S-RIP). *Atmos. Chem. Phys.*, *17*(23), 14593–14629. https://doi.org/10.5194/acp-17-14593-2017

Manney, G. L., Allen, D. R., Krüger, K., Naujokat, B., Santee, M. L., Sabutis, J. L., Pawson, S., Swinbank, R., Randall, C. E., … Long, C. (2005). Diagnostic comparison of meteorological analyses during the 2002 Antarctic winter. *Mon. Wea. Rev.*, *133*(5), 1261–1278. https://doi.org/10.1175/MWR2926.1

Parker, W. S. (2016). Reanalyses and observations: What’s the difference?. *Bull. Am. Meteor. Soc.*, *97*(9), 1565–1572. https://doi.org/10.1175/BAMS-D-14-00226.1

Pawson, S., and Fiorino, M. (1998). A comparison of reanalyses in the tropical stratosphere. Part 1: thermal structure and the annual cycle. *Climate Dyn.*, *14*(9), 631–644. https://doi.org/10.1007/s003820050246

Pawson, S., and Fiorino, M. (1999). A comparison of reanalyses in the tropical stratosphere. Part 3: inclusion of the pre-satellite data era. *Climate Dyn.*, *15*(4), 241–250. https://doi.org/10.1007/s003820050279

Randel, W., Udelhofen, P., Fleming, E., Geller, M., Gelman, M., Hamilton, K., Karoly, D., Ortland, D., Pawson, S., … Wu, D. (2004). The SPARC intercomparison of middle-atmosphere climatologies. *J. Climate*, *17*(5), 986–1003. https://doi.org/10.1175/1520-0442(2004)017<0986:TSIOMC>2.0.CO;2

Rao, J., Yu, Y. Y., Guo, D., Shi, C. H., Chen, D., and Hu, D. Z. (2019). Evaluating the Brewer–Dobson circulation and its responses to ENSO, QBO, and the solar cycle in different reanalyses. *Earth. Planet. Phys.*, *3*(2), 166–181. https://doi.org/10.26464/epp2019012

Shen, C., Zha, J. L., Wu, J., Zhao, D. M., Azorin-Molina, C., Fan, W. X., and Yu, Y. (2022). Does CRA-40 outperform other reanalysis products in evaluating near-surface wind speed changes over China?. *Atmos. Res.*, *266*, 105948. https://doi.org/10.1016/j.atmosres.2021.105948

Shi, C., and Zhai, P. M. (2024). Changes in climatic features of Northeast China Cold Vortex as reflected by ERA5 and CRA-40. *Atmos. Res.*, *300*, 107233. https://doi.org/10.1016/j.atmosres.2024.107233

Wang, Z. X., Yan, S. R., Hu, J. G., Deng, J. C., Ren, R. C., and Rao, J. (2024). Representation of the stratospheric circulation in CRA-40 reanalysis: The Arctic polar vortex and the quasi-biennial oscillation. *Adv. Atmos. Sci.*, *41*(5), 894–914. https://doi.org/10.1007/s00376-023-3127-1

Wright, C. J., and Hindley, N. P. (2018). How well do stratospheric reanalyses reproduce high-resolution satellite temperature measurements?. *Atmos. Chem. Phys.*, *18*(18), 13703–13731. https://doi.org/10.5194/acp-18-13703-2018

Yang, J. X., Huang, M. T., and Zhai, P. M. (2021). Performance of the CRA-40/Land, CMFD, and ERA-Interim datasets in reflecting changes in surface air temperature over the Tibetan Plateau. *J. Meteor. Res.*, *35*(4), 663–672. https://doi.org/10.1007/s13351-021-0196-x

Yang, P. K., Bao, M., Ren, X. J., and Tan, X. (2023). The role of vortex preconditioning in influencing the occurrence of strong and weak sudden stratospheric warmings in ERA5 reanalysis. *J. Climate*, *36*(4), 1197–1212. https://doi.org/10.1175/JCLI-D-22-0319.1

Zhao, B., Zhang, B., Shi, C. X., Liu, J. W., and Jiang, L. P. (2019). Comparison of the global energy cycle between Chinese Reanalysis Interim and ECMWF reanalysis. *J. Meteor. Res.*, *33*(3), 563–575. https://doi.org/10.1007/s13351-019-8129-7

Zhao, D., Zhang, L. X., Zhou, T. J., and Liu, J. W. (2021). Contributions of local and remote atmospheric moisture fluxes to East China precipitation estimated from CRA-40 reanalysis. *J. Meteor. Res.*, *35*(1), 32–45. https://doi.org/10.1007/s13351-021-0083-5